

## Hyperdynamics: Accelerated Molecular Dynamics of Infrequent Events

Arthur F. Voter

*Theoretical Division, Los Alamos National Laboratory, Los Alamos, New Mexico 87545*

(Received 4 February 1997)

I derive a general method for accelerating the molecular-dynamics (MD) simulation of infrequent events in solids. A bias potential ( $\Delta V_b$ ) raises the energy in regions other than the transition states between potential basins. Transitions occur at an accelerated rate and the elapsed time becomes a statistical property of the system.  $\Delta V_b$  can be constructed without knowing the location of the transition states and implementation requires only first derivatives. I examine the diffusion mechanisms of a 10-atom Ag cluster on the Ag(111) surface using a 220  $\mu\text{s}$  hyper-MD simulation. [S0031-9007(97)03180-3]

PACS numbers: 68.35.Fx, 02.70.Ns, 71.15.Pd, 82.20.Db

The molecular-dynamics (MD) simulation method is a powerful tool, widely used in chemistry, physics, and materials science. A long-standing problem, however, is that MD is typically limited to a time scale of nanoseconds or less, so many processes of interest cannot be simulated directly.

For many systems, the dynamics can be characterized as a sequence of infrequent transitions from one potential basin ("state") to another. In these cases, longer time scales can be accessed using transition state theory (TST) [1,2], in which the state-to-state rate constant is approximated as the flux through a dividing surface separating the states. This flux is an equilibrium property of the system, so actual dynamics need not be performed. Implicit in TST is the assumption that successive crossings of the dividing surface(s) are uncorrelated. In reality, correlated crossings events can occur. If desired, dynamical corrections [2,3] can be applied via short-time trajectories initiated at the dividing surface.

For processes such as surface or bulk diffusion, TST often yields an excellent approximation to the exact rate, especially if the TST surface is chosen to coincide with the saddle plane (the hyperplane orthogonal to the unstable mode at the saddle point) to minimize recrossings. Even in the harmonic approximation, where the rate depends only on properties at the saddle point and the minimum [4], the typical errors in TST are still much smaller than those due to the approximate interatomic potential. Consequently, TST is used widely in solid-state systems, and is the foundation (implicitly or explicitly) for lattice-based kinetic Monte Carlo simulations [5].

However, the utility of TST in treating infrequent-event dynamics has always rested on two crucial assumptions: that one knows in advance what the different states of the system will be, and that one can construct reasonable dividing surfaces along the boundaries between these states (or can find all the saddle points). Often, however, knowledge of the states to which a system will evolve is incomplete or incorrect. In metallic surface diffusion, for example, surprisingly complex, concerted events have

been discovered only recently [6–8]. These mechanisms are too complicated to allow advance prediction of all possible transitions from a given overlayer configuration.

Here I present a different approach to the infrequent-event problem, suitable for solid-state systems. Beginning from the TST approximation, a method is derived for extending the time scale of MD simulations without any advanced knowledge of either the location of the dividing surfaces or the states through which the system may evolve. A bias potential ( $\Delta V_b$ ) is designed to raise the energy of the system in regions other than at the TST dividing surfaces. Dynamics on the biased potential leads to accelerated evolution from state to state, while the elapsed time becomes a statistical property of the system. The instantaneous gain (or "boost") in the rate at which time advances (relative to direct MD) depends exponentially on the bias potential.

This hyper-MD method was recently derived and demonstrated for a 2D model potential and for surface self-diffusion on a Ni(100) terrace with nine moving atoms [9]. Exploiting the fact that at a saddle point the lowest eigenvalue ( $\epsilon_1$ ) of the Hessian matrix ( $\mathbf{H}$ ) is negative,  $\Delta V_b$  in that study was a simple function that tended to zero as  $\epsilon_1$  went negative. For larger,  $N$ -atom systems, formation and diagonalization of  $\mathbf{H}$  becomes a serious computational bottleneck. Moreover, the fraction of phase space for which all eigenvalues of  $\mathbf{H}$  are positive decreases rapidly with  $N$ , making a simple function of  $\epsilon_1$  inadequate as a definition for  $\Delta V_b$ . This effect was observable even for the  $N = 9$  case [9].

This Letter addresses this issue of treating larger systems. A definition for  $\Delta V_b$  that provides significant boost for hundreds of atoms is constructed from the two lowest eigenvalues of  $\mathbf{H}$  and the projection of the gradient onto the lowest eigenvector of  $\mathbf{H}$ . I show how to compute this  $\Delta V_b$  and the necessary derivatives in  $N$ -scaling fashion *without ever constructing the Hessian*, so that implementation of the hyper-MD method requires only first derivatives of the interatomic potential, as for normal MD.

Consider a TST-obeying, one-dimensional system, characterized at time  $t$  by position  $x(t)$  and potential energy  $V(x(t))$ . (A more detailed, many-dimensional derivation is given elsewhere [9].) The TST flux expression for the escape from the present potential basin (state “A”) through a TST boundary at  $x = q$  is given by

$$k_{A \rightarrow}^{\text{TST}} = \langle |dx/dt| \delta(x - q) \rangle_A. \quad (1)$$

Here  $\delta(\dots)$  is a Dirac delta function and  $\langle \dots \rangle_A$  indicates a classical, canonical-ensemble average restricted to the configuration space of state A.

Now consider adding to  $V(x)$  the non-negative bias potential,  $\Delta V_b(x)$ , which is zero at the TST boundaries. The TST escape rate is enhanced because the biased well is not as deep as the original well. However, this modification preserves the ratio of the TST escape rates from A to any two adjacent states [9]. This is a crucial property, with the consequence that a trajectory on  $V(x) + \Delta V_b(x)$  will escape to a given adjacent state (say, B) with the correct relative probability. Because the system obeys TST, this trajectory will thermalize in state B. If, in turn, state B has a biasing potential, the system will again exhibit accelerated escape to a state adjacent to B, and so on. *At an accelerated pace, the system evolves from state to state in a sequence representative of the exact dynamics.* (I.e., the probability of any given sequence, e.g., A-B-A-C-D-E..., is exactly the same for the biased dynamics as for the exact dynamics.) I now present the corrected time scale for this accelerated evolution.

Manipulating Eq. (1) with standard importance-sampling techniques [10] gives

$$k_{A \rightarrow}^{\text{TST}} = \frac{\langle |dx/dt| \delta(x - q) \rangle_{A_b}}{\langle e^{\beta \Delta V_b(x)} \rangle_{A_b}}, \quad (2)$$

in which the averages are taken over the biased state,  $A_b$ . Here  $\beta = 1/k_B T$ , where  $k_B$  is the Boltzmann constant and  $T$  is the temperature. Because  $\Delta V_b = 0$  where  $\delta(x - q) \neq 0$ , the numerator in Eq. (2) has been simplified from  $\langle |dx/dt| \delta(x - q) \exp[\beta \Delta V_b(x)] \rangle_{A_b}$ . Consequently, the numerator is exactly the TST escape rate from the biased state. The averages in Eq. (2) can be evaluated using a trajectory on the biased potential, confined to state  $A_b$  by reflecting boundaries. In a thought experiment, the averages can be evaluated to arbitrary accuracy by making the trajectory extremely long. As shown previously [9], a simple definition for the time evolved per biased MD step ( $\Delta t_b$ ) is then obtained by requiring that the average time between escape attempts (reflections) is equal to the correct value, which is  $1/k_{A \rightarrow}^{\text{TST}}$ . This yields

$$\Delta t_{b_i} = \Delta t_{\text{MD}} e^{\beta \Delta V_b(x(t_i))}; \quad t_b = \sum_i^{n_{\text{tot}}} \Delta t_{b_i}, \quad (3)$$

where  $\Delta t_{\text{MD}}$  is the MD integration time step,  $n_{\text{tot}}$  is the total number of MD steps, and  $t_i$  indicates the time at the  $i$ th MD step. The total elapsed boosted time is  $t_b$ .

Equation (3) is the heart of the hyper-MD method. At each integration step, the  $t_b$  clock is advanced by  $\Delta t_{b_i}$ , which depends on the instantaneous strength of the bias potential. [Note that where  $\Delta V_b(x_i) = 0$ ,  $\Delta t_{b_i} = \Delta t_{\text{MD}}$ .] While individual values of  $\Delta t_{b_i}$  have little meaning, at long times, by construction,  $t_b$  converges on the correct result. What is a “long” time depends on the statistical properties of the time-dependent boost factor,  $e^{\beta \Delta V_b(x(t))}$ . If escape from a state requires so many steps that the average boost factor ( $\langle e^{\beta \Delta V_b(x)} \rangle_{A_b}$ ) is well approximated, individual escape times will be meaningful, exhibiting the proper exponential probability distribution [11]. In contrast, an aggressive choice for  $\Delta V_b$  may stimulate escape in so few steps that predicted escape times are very noisy. Then the time scale becomes meaningful only after many transitions. In either case, the escape-time estimates are unbiased and their errors are uncorrelated, so, from the central limit theorem, the relative error in  $t_b$  decreases as  $t^{-1/2}$ , even if every state is different.

The key to implementing the hyperdynamics is designing a computationally tractable definition for  $\Delta V_b$  that does not require advanced knowledge of the transition states. Formally,  $\Delta V_b$  must be zero at all the dividing surfaces, must not block rapid ergodic sampling within a state, and must not introduce TST-violating correlations among the transitions. In practice, these requirements need only be met to a good approximation (the saddle points are the most important regions), and candidate forms for  $\Delta V_b$  can be tested on benchmark systems. I show here that a viable approach is to base  $\Delta V_b$  on local properties of the potential via the gradient vector,  $\mathbf{g}$  [ $g_i \equiv \partial V(\mathbf{r})/\partial x_i$ , where  $x_i$  is a component of the  $3N$ -dimensional vector  $\mathbf{r}$ ], and Hessian matrix,  $\mathbf{H}$  [ $H_{ij} \equiv \partial^2 V(\mathbf{r})/\partial x_i \partial x_j$ ].

Although the definition of the best TST dividing surface is inherently nonlocal (requiring steepest-descent trajectories), Sevick, Bell, and Theodorou [12] have proposed a local definition: the set of points in  $\mathbf{r}$  space for which  $\epsilon_1 < 0$  and  $g_{1p} = 0$ , where  $g_{1p} = \mathbf{C}_1^\dagger \mathbf{g}$  is the projection of  $\mathbf{g}$  onto the lowest eigenvector ( $\mathbf{C}_1$ ) of  $\mathbf{H}$ . Near the saddle points this is an excellent approximation to the TST surface, and the same quantities [ $\epsilon_1(\mathbf{r})$  and  $g_{1p}(\mathbf{r})$ ] can be used to construct a good definition for  $\Delta V_b(\mathbf{r})$ . Taking a sine wave with barrier height  $h$  and period  $2\pi d$  [ $V^{\text{cos}}(x) = (h/2) \cos(x/d)$ ] as a representative potential for an activated process, I define  $\Delta V_b^{\text{cos}}(x)$  as that function of  $\epsilon_1(x)$  and  $g_{1p}(x)$  that exactly “cancels” this potential,

$$\Delta V_b^{\text{cos}} = h/2 [1 + \epsilon_1/(\epsilon_1^2 + g_{1p}^2/d^2)^{1/2}]. \quad (4)$$

I.e.,  $V^{\text{cos}}(x) + \Delta V_b^{\text{cos}}(x) = h/2$  for all  $x$ ; the energy everywhere is raised to that of the transition state. Because  $\epsilon_1$  and  $g_{1p}$  are scalars, Eq. (4) is readily applied to the  $3N$ -dimensional system. Setting  $2\pi d$  to a physically reasonable transition length (e.g., a nearest-neighbor distance) and taking  $h$  to be somewhat smaller than the lowest anticipated barrier in the system gives the desired behavior.

A second bias term provides a smoothly increasing repulsion between the two lowest eigenvalues when they differ by less than  $\Delta\epsilon_c$ . Defining  $q = (\epsilon_2 - \epsilon_1)/\Delta\epsilon_c$ ,

$$\Delta V_b^{\Delta\epsilon} = \begin{cases} a[1 - 3q^2 + 2q^3], & \text{if } \epsilon_2 - \epsilon_1 \leq \Delta\epsilon_c, \\ 0, & \text{if } \epsilon_2 - \epsilon_1 > \Delta\epsilon_c. \end{cases} \quad (5)$$

$\Delta\epsilon_c$  should be set smaller than  $\epsilon_2 - \epsilon_1$  for a typical saddle point in the system so  $\Delta V_b^{\Delta\epsilon} = 0$  in the saddle plane. This term compliments  $\Delta V_b^{\cos}$  in regions where  $g_{1p}$  passes through zero as  $\epsilon_2$  and  $\epsilon_1$  cross. It also improves the numerical stability of the algorithm for computing  $\epsilon_1$ ,  $\epsilon_2$ , and  $g_{1p}$ , which is described next.

While direct differentiation of  $\Delta V_b$  requires third derivatives of  $V(\mathbf{r})$ , I now present a method that requires only first derivatives. Because  $\mathbf{H}$  is the matrix of second derivatives, finding  $\epsilon_1$  is equivalent to minimizing the second derivative of  $V$  with respect to the direction of the vector  $\mathbf{s}$  along which the derivative is calculated. Replacing this derivative  $[\partial^2 V(\mathbf{r})/\partial \mathbf{s}^2]$  with its numerical approximation,

$$\epsilon^{\text{num}}(\mathbf{s}) = [V(\mathbf{r} + \eta\mathbf{s}) + V(\mathbf{r} - \eta\mathbf{s}) - 2V(\mathbf{r})]/\eta^2 \quad (6)$$

( $\eta$  is a small number), this minimization ( $\mathbf{s} \rightarrow \mathbf{s}_{\min}$ ) can be performed as a steepest-descent or conjugate-gradient search, requiring only first derivatives of  $V$ . For example,

$$\frac{\partial \epsilon^{\text{num}}}{\partial s_i} = [g_i(\mathbf{r} + \eta\mathbf{s}) - g_i(\mathbf{r} - \eta\mathbf{s})]/\eta, \quad (7)$$

where  $g_i$  and  $s_i$  are components of  $\mathbf{g}$  and  $\mathbf{s}$ , respectively. The vector  $\mathbf{s}$  can be initialized from a random vector, or using  $\mathbf{s}_{\min}$  from the previous hyper-MD step. At convergence, the eigenvector and eigenvalue within this numerical approximation are given by  $\mathbf{C}_1^{\text{num}} = \mathbf{s}_{\min}$  and  $\epsilon_1^{\text{num}} = \epsilon^{\text{num}}(\mathbf{s}_{\min})$ . Because  $\epsilon^{\text{num}}(\mathbf{s}_{\min})$  is stationary with respect to  $\mathbf{s}$ , the derivatives of  $\epsilon_1$  needed for the MD forces are simply

$$\frac{\partial \epsilon_1^{\text{num}}}{\partial x_i} = [\{g_i(\mathbf{r} + \eta\mathbf{s}) + g_i(\mathbf{r} - \eta\mathbf{s}) - 2g_i(\mathbf{r})\}/\eta^2]_{\mathbf{s}=\mathbf{s}_{\min}}. \quad (8)$$

The same procedure can be used to find  $\epsilon_2$ , by maintaining orthogonality to  $\mathbf{C}_1^{\text{num}}$  during the minimization. Note that this approach to the eigenvalue problem is related to the fictitious Lagrangian method used to diagonalize the Hamiltonian in electronic structure calculations [13]. However, in the present formulation, the eigenvalues are found without ever constructing the matrix.

The projected gradient needed for Eq. (4) could be computed as  $g_{1p} = \mathbf{C}_1^{\text{num}\dagger} \mathbf{g}$ , but this would not be easily differentiable. Instead, the minimization method is applied to the two matrices  $\mathbf{H} + \lambda \mathbf{g} \mathbf{g}^\dagger$  and  $\mathbf{H} - \lambda \mathbf{g} \mathbf{g}^\dagger$ , by minimizing

$$\epsilon_{\pm\lambda}^{\text{num}}(\mathbf{s}) = \epsilon^{\text{num}}(\mathbf{s}) \pm \lambda \left[ \frac{V(\mathbf{r} + \eta\mathbf{s}) - V(\mathbf{r} - \eta\mathbf{s})}{2\eta} \right]^2, \quad (9)$$

yielding vectors  $\mathbf{s}_{+\lambda}$  and  $\mathbf{s}_{-\lambda}$ , respectively. A good approximation to the square of  $g_{1p}$  is found from [14]

$$(g_{1p}^{\text{num}})^2 = [\epsilon_{+\lambda}^{\text{num}} - \epsilon_{-\lambda}^{\text{num}}]/2\lambda. \quad (10)$$

Because  $\mathbf{s}_{+\lambda}$  and  $\mathbf{s}_{-\lambda}$  are stationary, calculating the derivative of  $(g_{1p}^{\text{num}})^2$  with respect to atom coordinates proceeds as for  $\epsilon_1$ , by differentiating Eqs. (9) and (10). The approximate character of Eqs. (6) and (10) has no adverse impact on the biased-potential dynamics, because the MD forces are obtained from direct differentiation of the approximate forms. However, incomplete convergence of the minimizations introduces errors. Computing  $(\Delta V_b)$  and its derivatives scales as  $N$  (for finite-ranged potentials) if the number of required iterations is constant with  $N$ , as preliminary tests indicate.

To show this bias potential gives correct results in a realistic application, I simulate the diffusive motion of a Ag adatom on the Ag(100) surface at  $T = 400$  K using an embedded atom method (EAM) interatomic potential [15]. The simulation cell, periodic in  $x$  and  $y$ , with free boundaries in  $z$ , is expanded to the quasiharmonic lattice constant for  $T = 400$  K. Fifty-five moving atoms (the adatom and the top three substrate layers) are in contact with two deeper, nonmoving layers. The MD time step is  $\Delta t_{\text{MD}} = 2 \times 10^{-15}$  s and a Langevin thermostat with a coupling rate of  $2 \times 10^{12}$  s $^{-1}$  gives canonical sampling.

In this system, the adatom diffuses by both hop and substrate-exchange [6] events. From molecular statics, the barriers for these mechanisms are 0.542 eV (hop) and 0.555 eV (exchange), and the Hessian eigenvalues at the saddles are  $\epsilon_1 = -0.87$  eV/Å $^2$ ,  $\epsilon_2 = 0.39$  eV/Å $^2$  (hop) and  $\epsilon_1 = -0.54$  eV/Å $^2$ ,  $\epsilon_2 = 0.44$  eV/Å $^2$  (exchange). Using this information, the bias potential ( $\Delta V_b = \Delta V_b^{\cos} + \Delta V_b^{\Delta\epsilon}$ ) was parametrized with  $h = 0.3$  eV,  $d = 0.46$  Å,  $\Delta\epsilon_c = 0.4$  eV/Å $^2$ , and  $a = 0.6$  eV. A  $3.7 \times 10^6$ -step hyper-MD run gave an average boost of 1356, for a total time of  $9.89 \pm 0.5$   $\mu$ s. Each hyper-MD step required  $\sim 30$  times the computational work of a direct-MD step, so the net computational boost was 45. Rate constants computed from the observed 23 hop events and 16 exchange events [ $2.3 \pm 0.5 \times 10^6$  s $^{-1}$  (hop),  $1.6 \pm 0.4 \times 10^6$  s $^{-1}$  (exchange)] are in agreement with the full harmonic (Vineyard [4]) rates of [ $2.84 \times 10^6$  s $^{-1}$  (hop),  $1.84 \times 10^6$  s $^{-1}$  (exchange)].

The second demonstration is for a more complex system: a 10-atom Ag cluster on the Ag(111) surface at  $T = 300$  K. Setting  $h = 0.3$  eV,  $\Delta\epsilon_c = 0.2$  eV/Å, and  $a = 0.4$  eV, and allowing two free layers (70 atoms moving), the procedure is otherwise as described above for the (100) face. [Note that this  $\Delta V_b$  would be inappropriately strong for a single adatom on Ag(111), for which the diffusion barrier is less than 0.1 eV [16].] Over a run for  $t_b = 221.2$   $\mu$ s, the average boost ratio was 8310. Although the cluster does not move far on this time scale, three distinct mechanisms are observed.

At  $9.5 \mu\text{s}$ , all 10 atoms jump in the same direction to move the cluster from hcp to fcc registry [Figs. 1(a) and 1(b)], a mechanism seen in simulations of crystal growth [7] and cluster motion [8,17]. This occurred many times, with the jump direction essentially always perpendicular to the long axis of the cluster. At the saddle point the cluster is rotated about  $8^\circ$ , allowing the atoms at one end of the cluster to remain close to perfect hcp positions while atoms at the other end come close to perfect fcc positions. For the other two jump directions, cluster rotation causes the atoms at the ends of the cluster to deviate unfavorably from their ideal paths; these saddles exhibit less rotation and are at higher energy.

At  $94.5 \mu\text{s}$ , the cluster breaks out of its compact configuration, allowing adatom motion at the cluster periphery [Figs. 1(c)–1(f)], as occurs on Ag(100) [15]. A few of the initiation events [Fig. 1(c)  $\rightarrow$  Fig. 1(d)] were observed, but usually the cluster returned immediately to the compact form. These periphery jumps are fast, with barriers of  $\sim 0.3 \text{ eV}$ , causing concern that the bias potential (with  $h = 0.3 \text{ eV}$ ) might be too strong for an accurate description of this section of the trajectory. However, tests with  $h = 0.2 \text{ eV}$  showed no qualitative difference in the behavior.

At  $197.8 \mu\text{s}$  [Figs. 1(g)–1(i)], there is a dislocation event (a mechanism discovered by Hamilton *et al.* [8]), resulting in a rotation of the cluster orientation and a change from hcp to fcc registry. This event, coupled with the hcp-to-fcc jump [Figs. 1(a) and 1(b)], may be a primary pathway for net translation at  $T = 300 \text{ K}$ .

In general applications, where the mechanisms are truly unknown, a lower bound on the lowest barrier height can

be estimated from the length of a direct MD simulation that shows no events at a given temperature. Choosing  $h$  lower than this barrier estimate, and taking a conservative (small) value for  $\Delta\epsilon_c$ , should give a “safe” bias potential. If necessary,  $h$  can be increased until events occur by applying this procedure iteratively, using hyper-MD to set successively higher bounds on the barrier. However, as the system evolves, one must watch for qualitative changes that may be accompanied by the onset of new, lower-barrier mechanisms, such as the cluster periphery diffusion seen above.

To summarize, the hyper-MD method appears promising, offering a way to extend the MD time scale by 2 or more orders of magnitude for strongly coupled, infrequent-event systems. It operates in continuous space (requiring no lattice mapping) and reduces to direct MD as  $\Delta V_b \rightarrow 0$ . Without prior knowledge of the transition state surfaces, an efficient bias potential can be constructed from local properties of  $V$  (based on  $\mathbf{H}$  and  $\mathbf{g}$ ), while implementation requires only first derivatives of  $V$ .

I am grateful for stimulating discussions and comments on the manuscript from J. Kress, P. Davids, W. Windl, S. Valone, and F. Houle, and for support from the Los Alamos LDRD program.

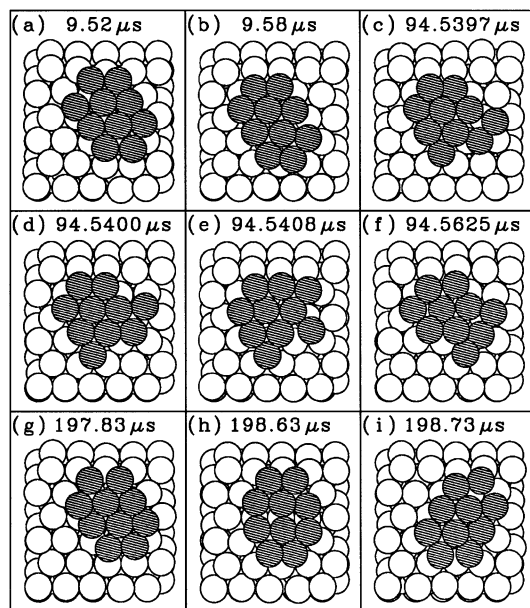


FIG. 1. Snapshots from  $\text{Ag}_{10}/\text{Ag}(111)$  hyper-MD simulation, discussed in text. Boosted time values ( $t_b$ ) are shown.

- 
- [1] R. Marcelin, *Ann. Phys.* **3**, 120 (1915).
  - [2] J. B. Anderson, *Adv. Chem. Phys.* **91**, 381 (1995).
  - [3] A. F. Voter and J. D. Doll, *J. Chem. Phys.* **82**, 80 (1985).
  - [4] G. H. Vineyard, *J. Phys. Chem. Solids* **3**, 121 (1957).
  - [5] A. F. Voter, *Phys. Rev. B* **34**, 6819 (1986).
  - [6] P. J. Feibelman, *Phys. Rev. Lett.* **65**, 729 (1990); G. L. Kellogg and P. J. Feibelman, *Phys. Rev. Lett.* **64**, 3143 (1990).
  - [7] M. Villarba and H. Jónsson, *Phys. Rev. B* **49**, 2208 (1994).
  - [8] J. C. Hamilton, M. S. Daw, and S. M. Foiles, *Phys. Rev. Lett.* **74**, 2760 (1995).
  - [9] A. F. Voter, *J. Chem. Phys.* **106**, 4665 (1997).
  - [10] J. P. Valleau and S. G. Whittington, in *Modern Theoretical Chemistry*, edited by B. J. Berne (Plenum, New York, 1977), Vol. 5, p. 137.
  - [11] Escape from the biased state obeys first order kinetics, so its escape time probability distribution is an exponential. A perfectly sampled boost factor simply rescales the time to recover the correct exponential distribution for the unbiased state.
  - [12] E. M. Sevick, A. T. Bell, and D. N. Theodorou, *J. Chem. Phys.* **98**, 3196 (1993).
  - [13] R. Car and M. Parrinello, *Phys. Rev. Lett.* **55**, 2471 (1985).
  - [14] A. F. Voter (to be published).
  - [15] A. F. Voter, in *Modeling of Optical Thin Films*, edited by M. R. Jacobson [*Proc. SPIE* **821**, 214 (1987)].
  - [16] C. L. Liu, J. M. Cohen, J. B. Adams, and A. F. Voter, *Surf. Sci.* **253**, 334 (1991).
  - [17] C. L. Liu and J. B. Adams, *Surf. Sci.* **268**, 73 (1992).